Evaluation of Energy Maximising Control Systems for Wave Energy Converters Using OpenFOAM®

Josh Davidson, Christian Windt, Giuseppe Giorgi, Romain Genest and John V. Ringwood

Abstract Wave energy conversion is an active field of research, aiming to harness the vast amounts of energy present in ocean waves. An essential development trajectory towards an economically competitive wave energy converter (WEC) requires early device experimentation and refinement using numerical tools. OpenFOAM® is proving to be a useful numerical tool for WEC development, having been increasingly employed in recent years to simulate and analyse the performance of WECs. This chapter reviews the latest works employing OpenFOAM® in the field of wave energy conversion, and then presents the new application, of evaluating energy maximising control systems (EMCSs) for WECs, in an OpenFOAM® numerical wave tank (NWT). The advantages of using OpenFOAM® for this application are discussed, and implementation details for simulating a controlled WEC in an OpenFOAM® NWT are outlined. An illustrative example is given, and results are presented, highlighting the value of evaluating EMCSs for WECs in an OpenFOAM® NWT.

1 Introduction

Ocean waves represent an enormous renewable energy resource, however, economically harvesting this energy is a challenging problem. Developing a cost-effective WEC requires early optimisation and refinement of the device's design and operation using numerical tools, before considering the expense of physical prototype construction, deployment and experimentation. An EMCS can greatly improve the performance of a WEC, without any substantial increase in capital costs. Therefore, optimising and refining a WEC design and operation, requires evaluating EMCSs using numerical tools.

Numerically analysing and simulating the fluid–structure interaction (FSI) between a WEC and its environment, requires solving the Navier–Stokes equations, a problem computationally infeasible for historic computers. Therefore, the equations were linearised to obtain results using boundary element methods (BEMs).

J. Davidson (✉) · C. Windt · G. Giorgi · R. Genest · J. V. Ringwood
Centre for Ocean Energy Research, Maynooth University, Maynooth, Ireland
e-mail: josh.davidson@nuim.ie

J. M. Nóbrega and H. Jasak (eds.), *OpenFOAM®*,
https://doi.org/10.1007/978-3-319-60846-4_12

The underlying hydrodynamics are based on linear potential theory, with assumptions of small wave and body motion amplitudes, inviscid fluid and an irrotational flow. However, these linearising assumptions are challenged by realistic WEC operation under *controlled* conditions. An EMCS effectively tunes the WEC dynamics to resonate with the incident waves, resulting in increased amounts of absorbed energy due to larger WEC motions. The large amplitude motions result in viscous drag, flow separation, vortex shedding and other nonlinear hydrodynamic effects.

Simulating a WEC under *controlled* conditions, therefore requires a realistic simulation environment, such as computational fluid dynamics (CFD). The discrepancy between the linear hydrodynamic model and CFD simulations, for WEC motions when the input wave frequencies are in the vicinity of the WEC resonant frequency, is shown by [48]. The output power estimations from the linear hydrodynamic model simulations, for frequencies around the WEC resonance, were shown to be considerably larger than the CFD estimations, due to the absence of viscous damping effects. The rigorous numerical treatment of the Navier–Stokes equations provided by CFD, enables a realistic, high- fidelity simulation environment for assessing WEC operation. However, the inclusion of nonlinear terms, neglected by linear hydrodynamic models, comes at the expense of massively larger computational requirements. Yet, the continuous improvement in performance and reduction in the cost of high-performance computers (HPCs), opens the way for CFD-simulated WEC experiments with reasonable computation times.

1.1 Outline of Chapter

This chapter focuses on the role OpenFOAM® can play in the evaluation of an EMCS for a WEC. OpenFOAM® provides open-source CFD solvers, whose application towards numerical experimentation on WEC devices has been rapidly growing in recent years. Section 2 reviews the usage of OpenFOAM® in wave energy research, showing a broad range of different WEC devices, simulated for a wide variety of research purposes. The new application of EMCS evaluation is then outlined in Sect. 3. A case study highlighting the importance of using a fully nonlinear simulation, such as OpenFOAM®, when evaluating the performance of an EMCS, is then presented in Sect. 4. The illustrative example in the case study, provides a comparison between the simulated motions and energy output of a WEC, under both *controlled* and *uncontrolled* conditions, calculated with a traditional linear hydrodynamic model and an OpenFOAM® simulation. An EMCS is used to drive a WEC into resonance with an incident wave field, and a divergence between the calculated linear model response and the OpenFOAM® simulation is observed.

2 OpenFOAM® in Wave Energy Applications

An extensive literature review of OpenFOAM®'s application in wave energy-related studies was presented in [6]. However, in the relatively short time since this review was composed (2015), numerous further studies have been published, demonstrating the growing usage of OpenFOAM® in wave energy research. This section builds upon [6], to provide an updated review detailing the broad range of WEC types and analysis purposes of OpenFOAM® in wave energy applications.

Oscillating water column (OWC)-type WECs operate by converting wave energy into pneumatic energy, whereby wave oscillations change the water levels inside of a chamber to force entrapped air through a turbine. OpenFOAM® is a useful tool for this type of WEC, able to model both the water and the air components of the OWC. Iturrioz et al. [24] validates an OpenFOAM® model for an OWC against physical experiments, showing excellent agreement among the free surface elevation (FSE), air pressure and velocity measurements. Likewise, [44–46] validate OpenFOAM® models of fixed OWCs against experimentally measured FSE and pressure data. To investigate the causes of damage to the Mutriku OWC plant, [29] use OpenFOAM® experiments to calculate flows, pressures and resulting loads at critical positions within the OWC.

An operating principle similar to that of an OWC is the *Blow Jet* WEC, which uses a horizontally oriented funnel to reproduce the hydraulic behaviour of a blowhole, turning relatively small waves into very strong air–water jets to drive an impulse turbine. Mendoza et al. [30] used OpenFOAM® to analyse different *Blow Jet* WEC configurations, validating results against measured pressure data. The *Bombora* WEC is comprised of submerged flexible membranes that use the force of incoming waves to drive air through a unidirectional air turbine. King et al. [26] uses an OpenFOAM® framework to model the FSI in the submerged flexible membranes of the *Bombora* WEC, coupling a simplified Finite Element model for the membrane and a thermodynamic model of the air ducting and turbine, with a CFD model for the water.

An oscillating wave surge converter (OWSC) is a flap-type WEC that rotates around a fixed axis in response to forcing from the incident waves. This type of WEC presents a particular meshing challenge in CFD, due to the large rotational displacements of the oscillating flap. A method for modelling this type of WEC in OpenFOAM® is presented in [42], along with a comparison of simulation results against experiments. The OpenFOAM® model developed in [42] is then used in [41] to optimise the power take-off (PTO) damping torque for a generic flap-type OWSC. Loh et al. [28] model a specific OWSC device, the *WaveRoller*, at a 1:24 scale under operational wave conditions to validate the numerical data with experiments. Ferrer et al. [16] model the *Oyster*, OWSC device, in extreme sea states to investigate slamming events, using both compressible and incompressible solvers, and compare the results against experiments. Akimoto et al. [1] proposes a new concept of rotational WEC, for capturing the orbital fluid particle motion of a wave. The preliminary CFD analysis demonstrates the rotating WEC and the wave flow field can keep the suitable position for torque generation in all the phases of orbital motion. Similarly, [13] implements

a 2D OpenFOAM® model for a quantitative investigation of the conversion performance of the *Seaspoon* WEC, which uses the same rotational operating principles.

Point absorber WECs are wave-activated bodies that are physically small compared to the typical wavelengths. OpenFOAM® was employed in [27, 31] to examine two-body self-reacting point absorber-type WECs, and in [35] to study the 'damper plate' component of self-reacting point absorbers. Devolder et al. [11] validates a heaving point absorber against free decay, and regular wave, experiments in a wave flume. Palm et al. [33] analyses a moored point absorber, by coupling a solver for the mooring system dynamics with OpenFOAM®, presenting the formulation for the coupled mooring analysis and validation results against physical experiments. Rafiee and Fiévez [34] uses OpenFOAM®, as well as traditional linear hydrodynamic models, to simulate the performance of the *CETO* point absorber WEC, under moderate and extreme wave conditions. The results in [34] were compared against physical experiments, showing a good agreement with the OpenFOAM® simulations but not by the linear models. Eskilsson et al. [14] investigates simulating the wave-induced motions of point absorber-type WECs, comparing the results of approximate but computationally efficient hydrodynamic models against the more complete but time-consuming OpenFOAM® simulations. Similarly, [17] investigate the difference among the performances of various linear and nonlinear hydrodynamic models compared with OpenFOAM® results, for the case of a heaving point absorber-type WEC.

The Ph.D. theses [4, 38], and the resulting papers, focus on the OpenFOAM® modelling of WECs. In [38], the use of OpenFOAM® to simulate WEC and mooring performance under survival sea conditions is investigated. The thesis presents several case studies; a fixed truncated cylinder, a moored buoy [36], the Wavestar [37] and Seabased WEC prototypes, including validation against physical wave tank experiments. Chen [4] implements wave generation and absorption by modifying the *interDyMFOAM* solver, and validates wave propagation and impact cases. The modified solver is then used to simulate and analyse the wave-induced roll motion of a rectangular barge and the hydrodynamic performance of an OWSC [5].

OpenFOAM® has been used for system identification of WEC models. The general concept of identifying mathematical models describing the dynamical behaviour of WECs from recorded data, using OpenFOAM® simulations as examples, is given in [40]. The types of identification tests available in an OpenFOAM® NWT are investigated in [10], and are used in [22] to identify the parameters of nonlinear hydrodynamic models. Giorgi and Ringwood [20] investigates the identification of hydrodynamic drag coefficients from OpenFOAM® experiments, the drag coefficients for the CETO WEC are identified by [34] using prescribed motion tests, and [2] determine nonlinear damping coefficients for a flap-type OSWC using free decay tests. Davidson et al. [7] uses system identification techniques to adapt the parameters of a linear control model online from measured responses of the WEC behaviour, so as to ensure the best linear model representation of the nonlinear conditions in the OpenFOAM® simulation.

Devolder et al. [12] review the *interDyMFoam* solver for the application of simulating a heaving buoy, outlining the importance of the fluid and body solver coupling

for wave energy applications and describe some pitfalls in the implemented methodology. Windt et al. [47] outlines an assessment methodology for the different numerical wavemakers available in an OpenFOAM® NWT for wave energy experiments, showcasing evaluation tests and metrics for their wave generation and absorption capabilities.

3 Evaluating Energy Maximisation Control Systems

By increasing the energy capture of a WEC, across changing sea states, EMCSs can improve the economic viability of the WEC. In addition to maximising energy output, EMCSs can also enforce constraints on the WECs operation. Maximum displacements and PTO forces can be constrained below desired values, so as to decrease device damage and fatigue and ensure efficient PTO sizing. A review of EMCSs for wave energy conversion is given in [39].

Evaluating the performance of an EMCS classically relied on linear model simulations. However, the increased amplitude of the WECs dynamics under controlled conditions challenges the validity of the linearising assumptions such models are built upon. Consistent with the observations in [48], the results in [9] show that increasing the amplitude of the WECs operation away from its zero-amplitude equilibrium state, leads to a divergence between the linear hydrodynamic model and CFD simulations. Specifically, the levels of hydrodynamic damping experienced by a WEC are seen to increase as the amplitude of operation increases. Therefore, evaluating an EMCS with a linear model will likely result in predictions of unrealistically large WEC motions and energy capture, due to an underestimation of the hydrodynamic damping on the WEC. CFD, on the other hand, has a greater range of validity when simulating large amplitude WEC motions. The treatment of nonlinear effects, such as viscosity or a time-varying wetted body surface area, enables CFD to provide a higher fidelity simulation, compared to a linear hydrodynamic model, at these operational amplitudes.

A strong advantage in choosing OpenFOAM® for the CFD simulation platform is the open-source nature of the software. The cost of commercial licenses can be prohibitive for university-based researchers, and WEC developers in small companies, with limited funds, which could be better spent purchasing HPC hardware or computing time. The open-source nature of OpenFOAM® often results in useful toolboxes being freely shared, a prime example being the wave generation and absorption toolboxes: waves2FOAM [25] and IHFOAM [23]. Of the papers reviewed in Sect. 2, waves2FOAM is used by [1, 10, 13, 19, 27, 30, 31, 34, 40, 43] and IHFOAM by [12, 24].

The complete access to the source code, provided by OpenFOAM®, allows modifications to be made. For example, mooring forces are applied to a WEC in [33] by modifying the *restraints* function in the *sixDoFRigidBodyMotion* solver, following the procedure outlined in [32]. The same function is modified in [10] to apply generic PTO forces to a WEC, and then is coupled with MATLAB in [7] to calculate opti-

mal control of the PTO force, as well as online system identification for the control model. Giorgi and Ringwood [19] implements latching control for a heaving sphere in regular waves where the WEC is 'latched' stationary during certain instants of the wave cycle, and then released at a later time when the phase of the incident wave is more favourable for increased energy capture. To implement the latching control, the source code was modified as detailed in [18].

4 Illustrative Example

An illustrative example is given, demonstrating the influence of the chosen simulation environment on the evaluation of an EMCS. Consider the WEC shown in Fig. 1, comprising a spherical buoy that acts as a point absorber. The WEC reacts against the inertia of the seafloor (or stationary damper plate) to extract power through a PTO force, F_{PTO}. Simulation of the WEC operation in an irregular sea state is performed by both an OpenFOAM® NWT and a linear hydrodynamic model, to compare the calculated wave-induced heave motion, $x(t)$, and energy capture

$$E(t) = \int_0^T F_{PTO}(t)\dot{x}(t)dt. \tag{1}$$

An *uncontrolled* case shall be used as a reference, in which the PTO acts as a simple linear damper, applying a purely resistive force proportional and opposite to the WEC velocity

$$F_{PTO}(t) = -d\dot{x}(t), \tag{2}$$

where d is the PTO damping parameter.

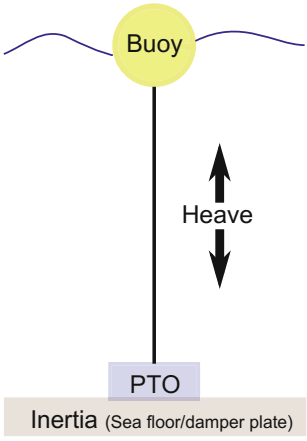

Fig. 1 WEC device considered in the illustrative example

The EMCS to be evaluated is PI control, which also applies a resistive PTO force proportional and opposite to the WEC velocity to absorb power, however, an additional reactive PTO force, proportional to the WECs displacement, is applied

$$F_{PTO}(t) = -d\dot{x}(t) - cx(t), \tag{3}$$

where c is the PTO spring parameter. PI control uses the reactive force to drive the WEC into resonance with the input waves, leading to increased WEC motions and energy capture. The value of c required to align the resonant period of the WEC, T_{WEC}, with the peak period of the input wave spectrum, T_p, is estimated here using linear oscillation theory, [15]

$$c = \frac{kT_{WEC}^2}{T_p^2} - k, \tag{4}$$

where k is the hydrodynamic restoring force coefficient.

The PTO damping parameter, d, is chosen as equal to the value of the WECs hydrodynamic radiation damping parameter at T_p, representing impedance matching at the peak wave period T_p [15].

4.1 Implementation

The illustrative example evaluates an EMCS, using both OpenFOAM® NWT and classical linear hydrodynamic model simulations. Here, implementation details, for the OpenFOAM® NWT, linear hydrodynamic model and EMCS, are given.

4.1.1 OpenFOAM® NWT

The implementation of the OpenFOAM® NWT is presented in [6]. The present example considers a WEC whose buoy has a radius of 0.1m, that floats 50% submerged at equilibrium, in the middle of a 100 m^2 square tank, with a 3 m water depth.

A cross-sectional view of the NWT mesh is depicted in Fig. 2a. Wave generation and absorption is implemented using the *waves2FOAM* toolbox and the wave creation and absorption zones are also depicted in Fig. 2a. In Fig. 2b, the dynamic pressure fields are seen to be generated in the wave creation zone, propagate through the central zone, interact with the WEC, and then be absorbed in the leeward side absorption zone. A unidirectional input wave spectrum, with a peak period of 1 s, is generated. The input waves are initially simulated without the WEC in the NWT, to allow the free surface elevation (FSE) to be measured at the centre of the tank. The FSE measurement is then used by the linear hydrodynamic model so that both simulations have the same input waves.

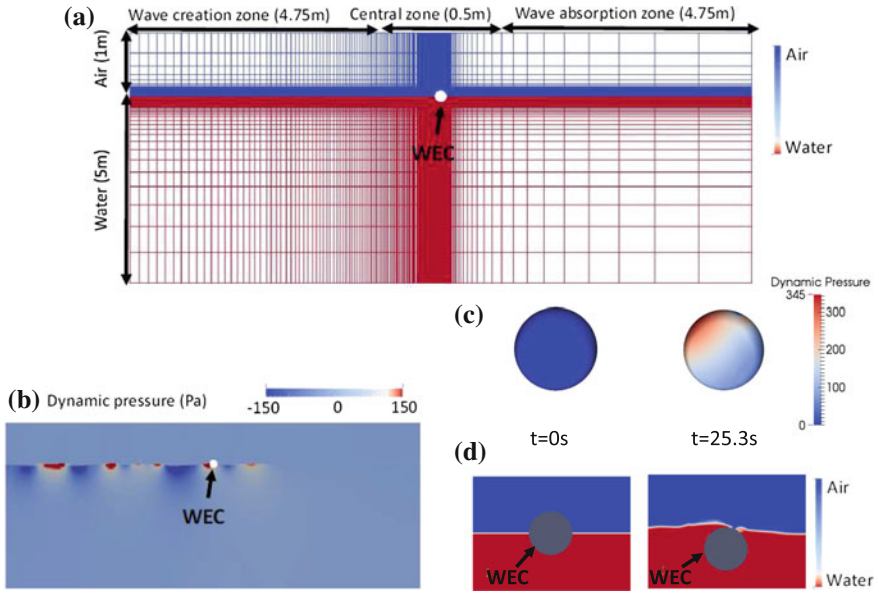

Fig. 2 Cross-sectional view of **a** the mesh and fluid volume fractions (water = red, air = blue) at time = 0 s, **b** the dynamic pressure at time = 25.3 s, **c** the dynamic pressure on the WEC at time = 0 s and 25.3 s, and **d** the fluid volume fractions around the WEC at time = 0 s and 25.3 s

4.1.2 Linear Model

The linear model, uses a fourth-order Runge–Kutta scheme to solve Cumin's equation, as described in [15], with the hydrodynamic parameters obtained from the open-source linear potential theory BEM software Nemoh [3].

4.1.3 Energy Maximising Controller

The PI controller is relatively easy to implement in OpenFOAM®, as it does not require any modifications to the source code. The *linearSpring* or *linearDamper* functions inside the *restraints* function of the *sixDoFRigidBodySolver* can be used directly. The functions require a *stiffness* and a *damping* value, which represent the PTO spring and damping parameters, c and d, in Eq. 3, respectively.

To determine the value for the PTO spring parameter, c, Eq. 4 can be used, once the values of T_{WEC} and k are known. To identify T_{WEC}, a free decay experiment is performed, Fig. 3a, and its spectral content is obtained, Fig. 3b, following the system identification techniques described in [10]. The peak of the spectrum in Fig. 3b, indicates a WEC resonant period of 0.61 s. To identify, k, the methods in [9] can be followed, using measurements of the hydrostatic force from the free decay experiment, Fig. 3c, to obtain the hydrostatic force versus displacement graph

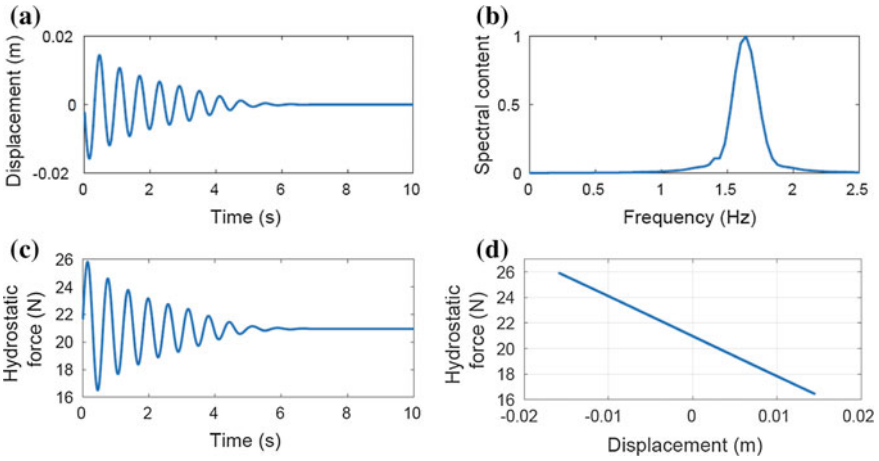

Fig. 3 **a** Simulated heave free decay test for WEC, **b** the spectral content of the signal indicating a resonant heave period of 0.61 s, **c** the hydrodstatic force versus displacement data used to identify the linear restoring force coefficient, and **d** system identification for the linear model's hydrostatic restoring force coefficient (method detailed in [9])

in Fig. 3d. The slope of the graph at $x = 0$ m, gives a linearised restoring force coefficient around the WEC equilibrium. A k value of 314 N/m can be identified from the results in Fig. 3d. Therefore, a PTO spring parameter, c, with a value of -197 N/m is obtained from Eq. 4. The PTO damping parameter, d, is set as equal to the linear hydrodynamic radiation damping at T_p, with a value of 6.22 Ns/m calculated using Nemoh.

4.2 Results

The generated input wave series is shown in Fig. 4a, the WEC heave motion for the uncontrolled and the PI control simulations are shown in Fig. 4b, c, respectively. The resulting heave motion for WECs using PI control can be seen to be considerably larger than for the uncontrolled cases. The absorbed energy is plotted in Fig. 4d, showing the effect of the reactive power applied by the PI controller, when during certain periods of time, the absorbed energy decreases, flowing back from the PTO to the WEC. However, over time, the PI-controlled WECs are seen to absorb considerably more energy than the uncontrolled WECs, highlighting the benefit of using control.

The results also show that the linear model and OpenFOAM® simulations agree well with each other in the uncontrolled case. However, in the controlled case, the linear model significantly overpredicts the WEC motion and absorbed energy compared to the higher fidelity OpenFOAM® simulation. At these larger amplitudes, nonlinear

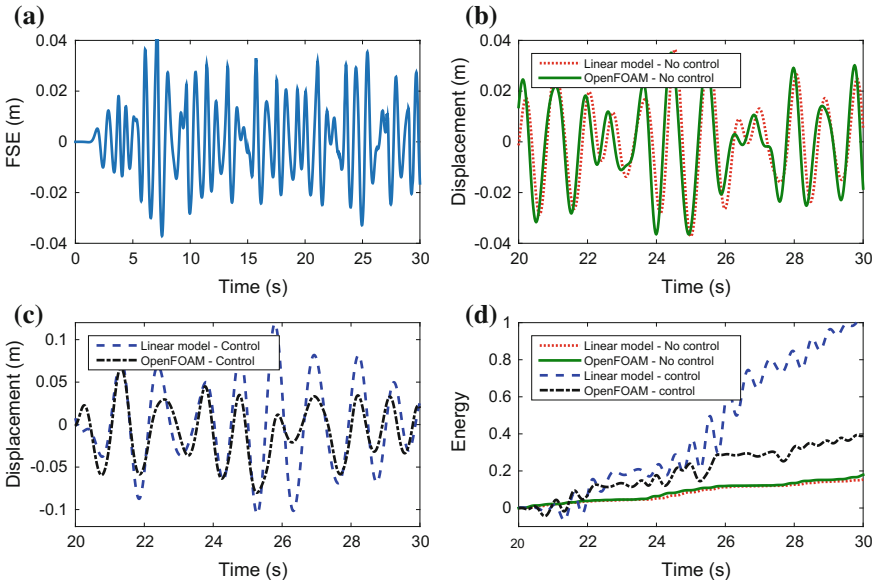

Fig. 4 **a** The measured FSE; **b** the heave displacement for the case of a passive damping PTO; **c** the heave displacement for the case of PI-controlled PTO; **d** normalised energy absorbed by the WEC

hydrodynamic effects begin to influence the device motion, and the predictions made by the linear model and the OpenFOAM® simulations diverge.

The operational space, in the displacement–velocity plane, spanned by the WEC motion is pictured in Fig. 5. The maximum WEC displacements and velocities from the four simulations in Fig. 4b, c are plotted. The operational space for the linear model and OpenFOAM® simulations of the uncontrolled WEC are very similar, and are much smaller than for the controlled WEC simulations. The linear model is seen to perform well compared to the more realistic OpenFOAM® simulation in the low amplitude operational space of the uncontrolled WEC. However, for the controlled WEC, the extended amplitude of the operational space diminishes the validity of the linear model, as nonlinear effects become relevant. Figure 5 shows that the operational space of the WEC motion in the OpenFOAM® simulation is much less than that predicted by the linear model simulation, likely due to the neglect of viscous drag effects by the linear model. The background of Fig. 5 displays a contour plot of the power absorbed by the PTO at each point in the operational space. The overprediction of absorbed energy made by the linear model for the controlled WEC, Fig. 4d, results from the WECs trajectory unrealistically spanning regions of large power absorption.

The amplitude of the relative displacement and relative velocity, between the WEC and the water, has a large effect on the presence of nonlinear hydrodynamic effects. For example, if the relative displacement between the WEC and the FSE

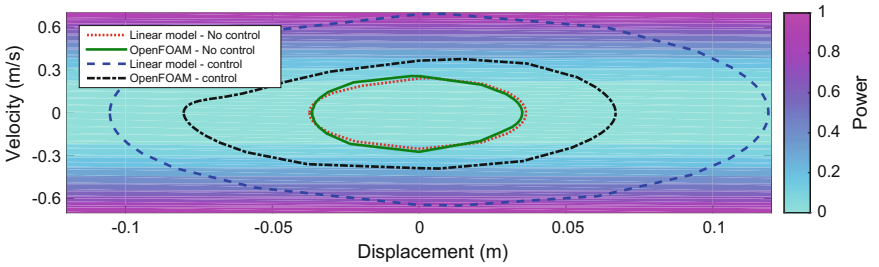

Fig. 5 The operational space in the displacement–velocity plane spanned by the WECs trajectory (lines), and the power absorbed by the PTO at each point in the operational space (contour)

exceeds the WEC radius, then the WEC will either be fully submerged or airborne. An example of that occurs at $t = 25.3$ s of the *controlled* OpenFOAM® simulation (shown in the snapshot of the WEC and the fluid in Fig. 2d). For a WEC geometry with a non-uniform horizontal cross section, such as the sphere, increasing the relative displacement amplitude increases the nonlinearity of the hydrodynamic restoring and Froude–Krylov forces, as shown in [8, 21], respectively. Viscous damping forces are dependent on the relative motion between the WEC and water, whereby viscous drag is often modelled as proportional to the square of the relative velocity.

The relative displacement between the WEC and the FSE is plotted in Fig. 6a, b, and the operational space, in the relative displacement–velocity plane, in Fig. 6c. The increase of different nonlinear hydrodynamic effects, for increasing amplitudes, are also indicated in Fig. 6c, and are seen to be more prevalent for a controlled WEC. Therefore, a realistic simulation environment, capable of modelling these nonlinear hydrodynamic effects, should be used when analysing the wave-induced motions of a WEC under *controlled* conditions.

While the illustrative example here utilised CFD, to capture the relevant nonlinear hydrodynamic effects evoked by the resulting large amplitude motions of a controlled WEC, other nonlinear hydrodynamic modelling techniques may also give improved results compared to the classical linear models, but with less computational requirements than CFD. A hierarchical approach to WEC hydrodynamic modelling is detailed in [14], examining the trade-off between model fidelity and computational requirements. Similarly, a comparison of different nonlinear hydrodynamic modelling techniques against the performance of an OpenFOAM® simulation is given in [17], for both an uncontrolled and a controlled WEC. Like the present illustrative example, the results in [17] also display a similar increase in operational space spanned by the uncontrolled and controlled WECs, and highlight the need for a high-fidelity nonlinear simulation environment for evaluating a controlled WEC.

The illustrative example shown, herein demonstrates the discrepancy between classical linear models and CFD when simulating a controlled WEC. To ensure confidence in the accuracy of the CFD results, the simulation should be validated against experimental data. Validating against a full-scale WEC in the open ocean is problematic, therefore a more common approach is to validate against a scaled-down

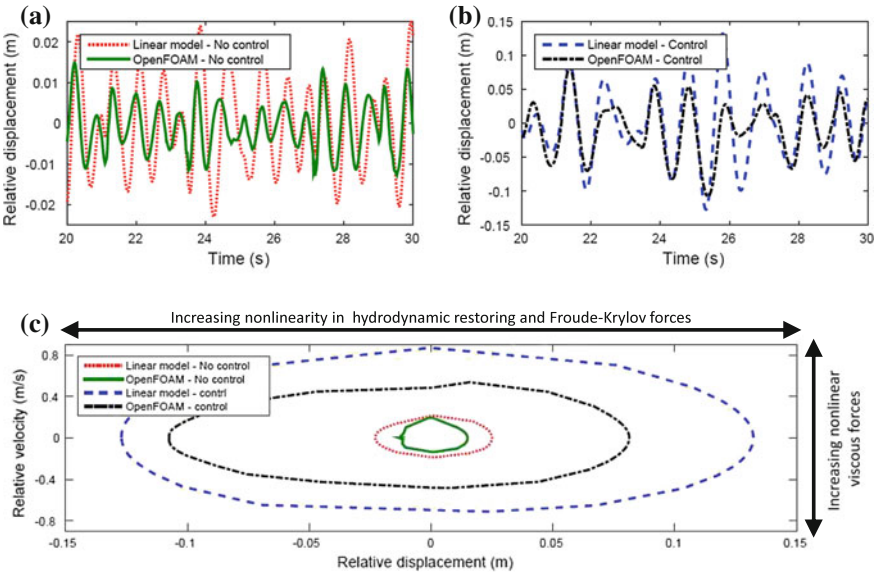

Fig. 6 The relative displacement between the WEC and FSE for **a** the uncontrolled WECs, and **b** the controlled WECs; **c** the relative displacement–relative velocity operational space spanned by the WEC trajectory

version of the WEC in an experimental wave tank facility, and then extrapolate that the validation holds true for full-scale conditions. The results from the illustrative example suggest that a CFD simulation validated under uncontrolled conditions will not extrapolate well to a simulation involving a controlled WEC, due the prevalence of nonlinear effects for the controlled WEC operation absent in the uncontrolled case.

5 Conclusion

Evaluating EMCSs for WECs requires an environment of realistic numerical simulation, capable of representing nonlinear hydrodynamic conditions. To maximise the absorbed energy, an EMCS will drive the WEC motion into resonance with an incident wave field, and the resulting FSI conditions challenge the validity of linear models. The example results shown in this chapter revealed that the energy capture evaluated by a linear model was more than double the energy predicted by the CFD simulation for a PI-controlled WEC. The increased amplitudes of the WEC displacement and velocity, and the relative WEC-water displacement and velocity, for a *controlled* WEC extend the operational space of the WEC dynamics far from the region where linear hydrodynamic assumptions are valid. The nonlinear FSI simula-

tions of CFD, on the other hand, are shown to more realistically handle the resonant conditions experienced when evaluating an EMCS for a WEC. OpenFOAM® is shown to be a useful simulation tool for the evaluation of an EMCS for a WEC.

Acknowledgements This chapter is based upon work supported by Science Foundation Ireland under Grant No. 13/IA/1886.

References

1. Akimoto, H., Kim, Y., Tanaka, K.: Configuration of the single-bucket wave turbine for the direct utilization of orbital fluid motion. In: Grand Renewable Energy (2014)
2. Asmuth, H., Schmitt, P., Elsaesser, B., Henry, A.: Determination of non-linear damping coefficients of bottom-hinged oscillating wave surge converters using numerical free decay tests. In: Proceedings of the 1st International Conference on Renewable Energies Offshore, Lisbon, Portugal, pp. 24–26 (2014)
3. Babarit, A., Delhommeau, G.: Theoretical and numerical aspects of the open source BEM solver NEMOH. In: 11th European Wave and Tidal Energy Conference (EWTEC2015) (2015)
4. Chen, L.: Modelling of marine renewable energy. Ph.D. thesis, University of Bath (2015)
5. Chen, L., Zang, J., Hillis, A.J., Plummer, A.R., et al.: Hydrodynamic performance of a flap-type wave energy converter in viscous flow. In: The Twenty-fifth International Offshore and Polar Engineering Conference. International Society of Offshore and Polar Engineers (2015)
6. Davidson, J., Cathelain, M., Guillemet, L., Le Huec, T., Ringwood, J.: Implementation of an OpenFOAM® numerical wave tank for wave energy experiments. In: Proceedings of the 11th European Wave and Tidal Energy Conference (EWTEC 2015), Nantes (2015)
7. Davidson, J., Genest, R., Ringwood, J.V.: Adaptive control of a wave energy converter simulated in a numerical wave tank. In: Proceedings of the 12th European Wave and Tidal Energy Conference (EWTEC 2017), Cork (2017)
8. Davidson, J., Giorgi, S., Ringwood, J.: Numerical wave tank identification of nonlinear discrete-time hydrodynamic models. In: 1st Int. Conf. on Renewable Energies Offshore (Renew 2014), Lisbon (2014)
9. Davidson, J., Giorgi, S., Ringwood, J.V.: Linear parametric models for ocean wave energy converters identified from numerical wave tank experiments. Ocean Engineering **103** (2015)
10. Davidson, J., Giorgi, S., Ringwood, J.V.: Identification of wave energy device models from numerical wave tank datapart 1: Numerical wave tank identification tests. IEEE Transaction on Sustainable Energy (2016)
11. Devolder, B., Rauwoens, O., Troch, P.: Numerical simulation of a single floating point absorber wave energy converter using OpenFOAM®. In: Proceedings of the 2nd International Conference on Renewable Energies Offshore (2016)
12. Devolder, B., Schmitt, P., Rauwoens, P., Elsaesser, B., Troch, P.: A review of the implicit motion solver algorithm in OpenFOAM® to simulate a heaving buoy. In: NUTTS conference 2015: 18th Numerical Towing Tank Symposium, pp. 1–6 (2015)
13. Di Fresco, L., Traverso, A., Barberis, S., Guglielmino, E., Garrone, M.: Off-shore wave energy harvesting: A wec-microturbine system: Harvesting and storing energy for off-shore applications. In: OCEANS 2015-Genova, pp. 1–6. IEEE (2015)
14. Eskilsson, C., Palm, J., Engsig-Karup, A., Bosi, U., Ricchiuto, M.: Wave induced motions of point-absorbers: a hierarchical investigation of hydrodynamic models. In: 11th European Wave and Tidal Energy Conference (EWTEC). Nantes, France (2015)
15. Falnes, J.: Ocean Waves and Oscillating Systems : linear interactions including wave-energy extraction. Cambridge University Press (2002)

16. Ferrer, P.M., Causon, D.M., Qian, L., Mingham, C.G., Ma, Z.H.: Numerical simulation of wave slamming on a flap type oscillating wave energy device. In: Proceedings of the Twenty-sixth (2016) International Ocean and Polar Engineering Conference (2016)
17. Giorgi, G., Retes, M., Ringwood, J.: Nonlinear hydrodynamic models for heaving buoy wave energy converters. In: 3rd Asian Wave and Tidal Energy Conference (2016)
18. Giorgi, G., Ringwood, J.: NWT Latching Control User Manual. Available at: http://www.eeng.nuim.ie/coer/doc/NWTLatchingControlUserManual.pdf
19. Giorgi, G., Ringwood, J.V.: Implementation of latching control in a numerical wave tank with regular waves. Journal of Ocean Engineering and Marine Energy **2**(2), 211–226 (2016)
20. Giorgi, G., Ringwood, J.V.: Consistency of viscous drag identification tests for wave energy applications. In: Proceedings of the 12th European Wave and Tidal Energy Conference (EWTEC 2017), Cork (2017)
21. Giorgi, S., Davidson, J., Ringwood, J.V.: Identification of nonlinear excitation force kernals using numerical wave tank experiments. In: EWTEC (2015)
22. Giorgi, S., Davidson, J., Ringwood, J.V.: Identification of wave energy device models from numerical wave tank data - part 2: Data-based model determination. IEEE Transaction on Sustainable Energy (2016)
23. Higuera, P., Lara, J.L., Losada, I.J.: Simulating coastal engineering processes with OpenFOAM®. Coastal Engineering **71**, 119–134 (2013)
24. Iturrioz, A., Guanche, R., Lara, J., Vidal, C., Losada, I.: Validation of OpenFOAM® for oscillating water column three-dimensional modeling. Ocean Engineering **107**, 222–236 (2015)
25. Jacobsen, N.G., Fuhrman, D.R., Fredsøe, J.: A wave generation toolbox for the open-source CFD library: OpenFOAM®. International Journal for Numerical Methods in Fluids **70**, 1073–1088 (2012)
26. King, A., Algie, C., Ryan, S., Ong, R.: Modelling of fluid structure interactions in submerged flexible membranes for the bombora wave energy converter. In: 20th Australasian Fluid Mechanics Conference, Perth, Australia (2016)
27. Li, L., Tan, M., Blake, J., et al.: Numerical simulation of multi-body wave energy converter. In: The Twenty-fifth International Offshore and Polar Engineering Conference. International Society of Offshore and Polar Engineers (2015)
28. Loh, T.T., Greaves, D., Maeki, T., Vuorinen, M., Simmonds, D., Kyte, A.: Numerical modelling of the WaveRoller device using OpenFOAM®. In: Proceedings of the 3rd Asian Wave & Tidal Energy Conference (2016)
29. Medina-Lopez, E., Allsop, W., Dimakopoulos, A., Bruce, T.: Conjectures on the failure of the OWC breakwater at Mutriku. In: Coastal Structures (2015)
30. Mendoza, E., Chávez, X., Alcérreca-Huerta, J.C., Silva, R.: Hydrodynamic behavior of a new wave energy convertor: The blow-jet. Ocean Engineering **106**, 252–260 (2015)
31. Mishra, V., Beatty, S., Buckham, B., Oshkai, P., Crawford, C.: Application of an arbitrary mesh interface for CFD simulation of an oscillating wave energy converter. In: Proc. 11th Eur. Wave Tidal Energy Conf, pp. 07B141–07B1410 (2015)
32. Palm, J.: Connecting OpenFOAM® with matlab. Online: http://www.tfd.chalmers.se/hani/kurser/OSCFD2012/ (2012)
33. Palm, J., Eskilsson, C., Paredes, G.M., Bergdahl, L.: Coupled mooring analysis for floating wave energy converters using CFD: Formulation and validation. International Journal of Marine Energy **16**, 83–99 (2016)
34. Rafiee, A., Fiévez, J.: Numerical prediction of extreme loads on the CETO wave energy converter. 11th European Wave and Tidal Energy Conference (EWTEC). Nantes, France (2015)
35. Rajagopalan, K., Nihous, G.: Study of the force coefficients on plates using an open source numerical wave tank. Ocean Engineering **118**, 187–203 (2016)
36. Ransley, E., Greaves, D., Raby, A., Simmonds, D., Hann, M.: Survivability of wave energy converters using CFD. Renewable Energy **109**, 235–247 (2017). https://doi.org/10.1016/j.renene.2017.03.003
37. Ransley, E., Greaves, D., Raby, A., Simmonds, D., Jakobsen, M., Kramer, M.: RANS-VOF modelling of the wavestar point absorber. Renewable Energy **109**, 49–65 (2017). https://doi.org/10.1016/j.renene.2017.02.079

38. Ransley, E.J.: Survivability of wave energy converter and mooring coupled system using CFD. Ph.D. thesis, Plymouth University, UK (2015)
39. Ringwood, J.V., Bacelli, G., Fusco, F.: Energy-maximizing control of wave-energy converters: the development of control system technology to optimize their operation. IEEE Control Systems **34**(5), 30–55 (2014)
40. Ringwood, J.V., Davidson, J., Giorgi, S.: Numerical Modeling of Wave Energy Converter: State-of-the-art techniques for single WEC and converter arrays, chap. Identifying models using recorded data. Elsevier (2016)
41. Schmitt, P., Asmuth, H., Elsäßer, B.: Optimising power take-off of an oscillating wave surge converter using high fidelity numerical simulations. International Journal of Marine Energy **16**, 196–208 (2016)
42. Schmitt, P., Elsaesser, B.: On the use of OpenFOAM® to model oscillating wave surge converters. Ocean Engineering **108**, 98–104 (2015)
43. Simonetti, I., Cappietti, L., El Safti, H., Oumeraci, H.: 3d numerical modelling of oscillating water column wave energy conversion devices: current knowledge and OpenFOAM® implementation. In: 1st International Conference on Renewable Energies Offshore (2014)
44. Simonetti, I., Cappietti, L., El Safti, H., Oumeraci, H.: Numerical modelling of fixed oscillating water column wave energy conversion devices: Toward geometry hydraulic optimization. In: ASME 2015 34th International Conference on Ocean, Offshore and Arctic Engineering, pp. V009T09A031–V009T09A031. American Society of Mechanical Engineers (2015)
45. Simonetti, I., Crema, I., Cappietti, L., El Safti, H., Oumeraci, H.: Site-specific optimization of an OWC wave energy converter in a Mediterranean area. In: Progress in Renewable Energies Offshore, pp. 343–350. CRC Press (2016)
46. Vyzikas, T., Deshoulieres, S., Giroux, O., Barton, M., Greaves, D.: Numerical Study of fixed Oscillatin Water Column with RANS-type two-phase CFD model. Renewable Energy **102**, 294–305 (2017)
47. Windt, C., Davidson, J., Schmitt, P., Ringwood, J.V.: Assessment of numerical wave makers. In: Proceedings of the 12th European wave and tidal energy conference (EWTEC 2017), Cork (2017)
48. Yu, Y.H., Li, Y.: Reynolds-averaged navier–stokes simulation of the heave performance of a two-body floating-point absorber wave energy system. Computers & Fluids **73**, 104–114 (2013)